



Science Arts & Métiers (SAM)

is an open access repository that collects the work of Arts et Métiers Institute of Technology researchers and makes it freely available over the web where possible.

This is an author-deposited version published in: <https://sam.ensam.eu>
Handle ID: <http://hdl.handle.net/10985/22718>

To cite this version :

Alexandre RONDEPIERRE, Yann ROUCHAUSSE, Laurent VIDEAU, Olivier CASAGRANDE, Olivier CASTELNAU, Laurent BERTHE - Laser interaction in a water tank configuration: Higher confinement breakdown threshold and greater generated pressures for laser shock peening - Journal of laser applications - Vol. 33, n°4, p.042022-1 042022-9 - 2021

Any correspondence concerning this service should be sent to the repository

Administrator : scienceouverte@ensam.eu



Laser interaction in a water tank configuration: Higher confinement breakdown threshold and greater generated pressures for laser shock peening

Alexandre Rondepierre,^{1,2,a)}  Yann Rouchausse,¹  Laurent Videau,^{3,4}  Olivier Casagrande,² Olivier Castelnau,¹ 
and Laurent Berthe¹ 

AFFILIATIONS

¹Laboratoire Procédés et Ingénierie en Mécanique et Matériaux (PIMM), UMR8006 ENSAM, CNRS, CNAM, 151 bd de l'Hôpital, 75013 Paris, France

³THALES LAS France, 78990 Elancourt, France

²CEA, DAM, DIF, 91297 Arpajon, France

⁴Laboratoire Matière en Conditions Extrêmes, Université Paris-Saclay, CEA, 91680 Bruyères-le-Châtel, France

^{a)}Electronic mail: alexandre.rondepierre@fr.thalesgroup.com

ABSTRACT

The authors present a new configuration for laser-induced plasmas in confined regimes for a 10 ns-range laser pulse in the green wavelength (532 nm) that repulses the breakdown threshold above 20 GW/cm² compared to 8 GW/cm² as generally indicated in previous works. Using this new configuration, pressures above 12 GPa have been reached for the first time in confined regimes. This can enlarge the range of applications of laser shock such as the range of treatable materials (very high strength materials) or facilities' costs since neither vacuum nor heavy laser systems will be needed to reach these levels of pressure. The proposed configuration mainly consists of the usage of a water tank. Hence, a great thickness of water is used instead of the extensively used thin water layer. Therefore, the water breakdown plasma will not initiate at the surface of the water, as the laser beam is still not focused there. Instead, it will occur in the depth of the water. In that case, the breakdown threshold value is increased as either the avalanche breakdown or the multiphoton ionization may start at higher laser intensities than at the air/water interface. The authors experimentally demonstrated this new breakdown threshold with the measurement of transmitted intensity, transmitted pulse duration, and the indirect measurement of the plasma pressure. Multiple shots (laser shock treatment) were also performed, and the specimen surface deformation was measured, leading to the same conclusion.

Key words: water breakdown, plasma breakdown, water tank configuration, VISAR analysis, pressure record, laser shock application

I. INTRODUCTION

An effective way of generating high pressures (>GPa) is to focus a high-power pulsed laser (1 J, 10 ns) on a metal target. The laser beam is then absorbed, and its energy is used to heat and to ionize the target. Then, the generated high-pressure plasma creates a strong shock wave inside the material. The technique can be used in many fields, such as surface treatments [laser shock peening—LSP (Ref. 1) and laser stripping²], nondestructive adhesion test [Laser Shock Adhesion Test—LASAT (Ref. 3)], or more

generally for physical experiments ranging from material characterization to space propulsion.⁴

At the beginning of the development of this process, the plasma was generating in the direct regime in which the laser is directly illuminating the specimen. After a while, the confined regime was developed by Anderholm.⁵ It consists of covering the metal target by a medium transparent to the laser (such as water, quartz, or polymers) in order to confine the plasma. As a consequence, it was demonstrated that the generated pressure can be

increased by four times and its duration by two times, compared to the direct regime at the same laser intensity.⁶

However, Berthe *et al.* demonstrated that the pressure cannot exceed 4–6 GPa in the confined regime⁷ (with 25 ns laser pulse duration at 1064 nm), since a breakdown plasma appears at the surface of the confinement layer. The mechanism behind the initiation and creation of that breakdown plasma is complex and shows that there is a balance between two phenomena: the MultiPhoton Ionization and the avalanche breakdown.⁸

The breakdown plasma absorbs the laser energy and screens the incident laser pulse. Hence, the plasma of interest for shock generation, located on the metal target, can no longer be heated by the laser for pressure generation. Therefore, it does not receive a higher laser intensity than the breakdown threshold intensity: there is a saturation.

This breakdown was experimentally studied for water confinement regime (WCR), and it was demonstrated that the occurrence threshold was ranging from 6 to 10 GW/cm²,⁸ even though it depends on many parameters such as laser wavelength⁹ or laser pulse duration.¹⁰

Sollier *et al.*¹¹ experimentally found a threshold of 6 and 10 GW/cm² for a 10 ns laser pulse in, respectively, green wavelength (532 nm) and infrared one (1064 nm), for a thin layer of water (a few mm), with a breakdown plasma located at the water surface. However, previous experimental results from Vogel *et al.*¹² estimated the threshold value to be around 30 GW/cm² for a 6 ns laser pulse at 532 nm, for a laser beam focused in a glass bowl filled with water. In addition, Zhang *et al.*¹³ used numerical simulations to calculate the breakdown threshold inside water and find the threshold value to be between 6 and 41 GW/cm² for a 6 ns laser pulse at 532 nm.

Hence, it appears that the breakdown threshold depends on whether a thin layer or a great thickness of water is used.

In this paper, we present a new configuration that is developed to repel the actual water breakdown threshold by two times its value for the same used laser parameters. The main aim of the proposed configuration is to suppress the breakdown plasma appearing at the surface of the water by decreasing the laser intensity at

the water/air interface. This was done by using a Water Tank Configuration (WTC) that moves the water breakdown phenomena inside the water instead of at the water surface. Indeed, as the beam is not focused while entering the water, the laser intensity remains low and no breakdown starts.

In the first part of this paper, we introduce the experimental setup used, and in the second part we present the results obtained via multiple experiments: energy transmission, laser pulse duration, and plasma pressure measurements.

These experiments have demonstrated the effectiveness of the WTC to generate the highest reported pressure for the water confined regime. We confirm these results in a third part with a configuration close to the LSP process.

II. EXPERIMENTAL SETUP

Experiments were conducted at the Hephaïstos laser facility, located in the PIMM laboratory (Procédés et Ingénierie en Mécanique et Matériaux) in Paris, France. A Thales GAIA HP laser was used. It consists of two symmetrical flashlamp-pumped Nd:YAG laser, with a pulse duration of 7.2 ns at a repetition rate of 2 Hz. As water absorption is high in the infrared range, the Nd:YAG pulse is frequency doubled into green wavelength (532 nm). Each beam can deliver up to 7 J at 532 nm, and they are combined for a total output of 14 J.

Laser spots were set from 1.5 to 3 mm diameter and smoothed by the use of a DOE (diffractive optical element). The phase of the input beam is then modified to obtain a homogeneous spatial distribution of intensity in the focal plane. Indeed, the laser propagates by more than 8 m (six meters between the source and the lens, and two more meters of equivalent propagation when imaging the beam into a 3 mm spot size with a +300 mm lens), and thus it experiences high-diffraction effects and over-intensities appear in the spatial profile if a DOE is not inserted (see Fig. 1).

The beam size at the water/air interface was greater than 10 mm so that the intensity will never exceed 1 GW/cm².

The laser pulse duration was measured with a DET10A2 (Thorlabs) photodiode. Energy transmissions were measured with

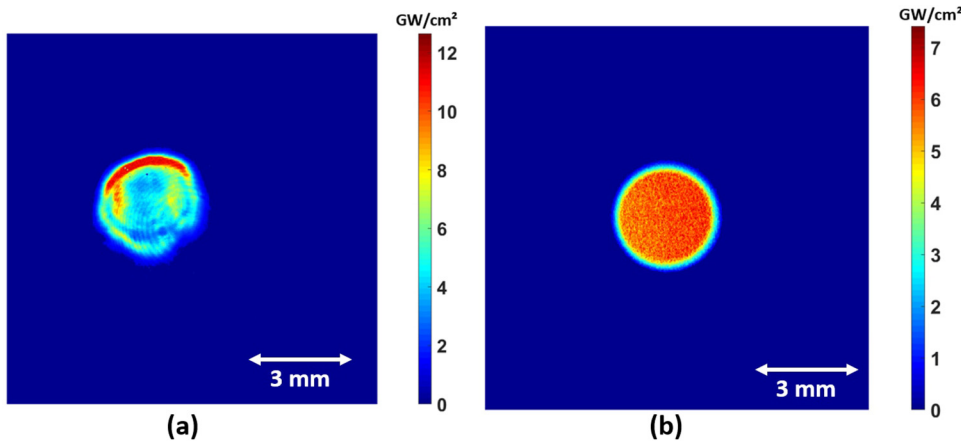


FIG. 1. Spatial distribution of intensity in the laser beam cross section at the focal point ($I_{\text{mean}} = 4 \text{ GW/cm}^2$) (a) without DOE and (b) with DOE.

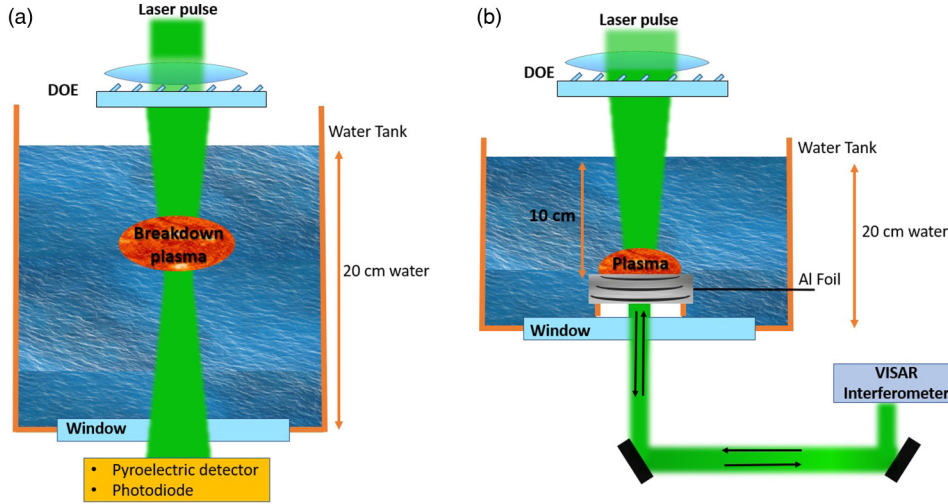


FIG. 2. Experimental diagnoses used with the Water Tank setup (right and left schemes are not at the same scale).

a Gentec-EO pyroelectric detector. Moreover, pressure measurements were conducted from rear surface velocity measurements obtained by the use of a VISAR (Velocity Interferometer System for Any Reflector). Pure aluminum (99.9%) was used for VISAR characterization.

A VISAR¹⁴ is an accurate optical tool, acting mainly like a radar, and constituted of two parts:

- A single (longitudinal) mode and continuous laser probe beam (Verdi 5W-532 nm, made by Coherent), which is focused on the rear surface of the sample being laser-shocked. This probe beam will be wavelength-shifted by Doppler-Fizeau effect when the plasma-generated shock wave reaches the rear surface of the specimen.
- The second part is a Michelsonlike interferometer used to analyze the wavelength shift. By analyzing the intensity within the interference fringes pattern, one can obtain the time-resolved rear velocity of the target.

The used water tank is designed with a transparent window at the laser wavelength (as represented in Fig. 2) to measure the light which is transmitted through the water (for energy and pulse duration measurements). We also used the same setup to measure the rear-free surface velocity of targets irradiated by the laser inside the water tank (for pressure measurements with VISAR).

Various focal lengths from +150 to +300 mm were used to set the focal spot size from 1.5 to 3 mm, and in each case, the focal plane was positioned about 10 cm under the water surface (Water Tank). The laser beam size before the lens was about 20 mm.

III. EXPERIMENTAL RESULTS AND DISCUSSIONS

The breakdown plasma initiation inside water was measured in different ways. When the breakdown occurs, the created plasma absorbs the remaining energy of the laser pulse so that the effective transmitted laser pulse is shortened, and its energy is reduced. Therefore, the transmission is measured (both in energy and in duration) to detect at which intensity the breakdown is starting.

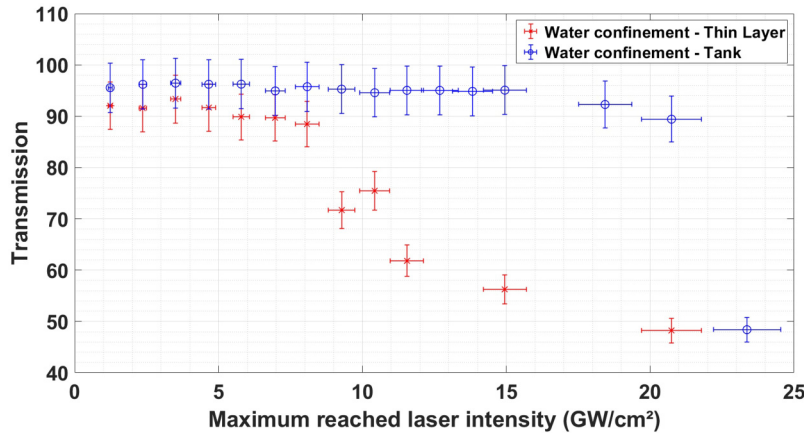


FIG. 3. Transmitted energy as a function of laser intensity for the two configurations: water tank and thin layer of water.

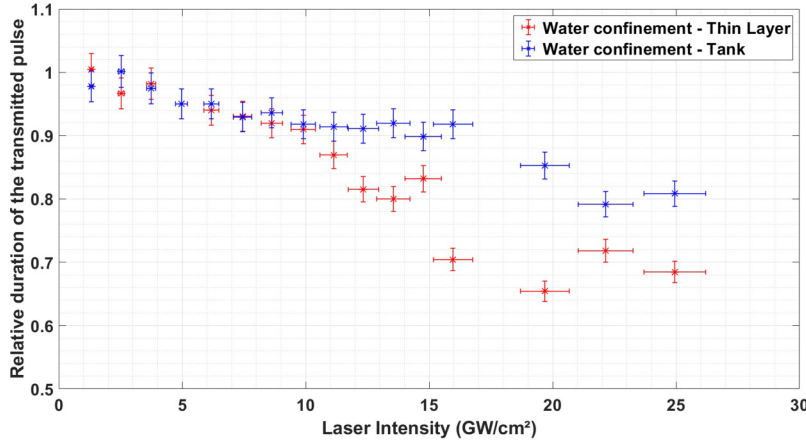


FIG. 4. FWHM of the laser pulse transmitted through water as a function of laser intensity for the two configurations. Data are relative to the FWHM of the laser pulse without any water (7.2 ns).

On the other hand, we performed pressure measurements by VISAR analysis. Since the generated pressure is related to the laser intensity [P (GPa) $\propto \sqrt{I}$ (GW/cm²)⁶], it will increase until we reach the breakdown. At that point, the effective intensity reaching the target saturates and the pressure stops increasing. Previous works^{15,16} stated that the threshold intensity at which the breakdown starts is around 8–10 GW/cm², and the saturated pressure is around 6–8 GPa.

A. Transmission measurements

The transmission as a function of the laser intensity (GW/cm²) is plotted in Fig. 3. It is defined as $T = E_t/E_i$, with E_i being the incident energy without water and E_t being the transmitted energy measured both with the WTC (the beam is focused ≈ 10 cm under the water surface) and with the thin layer of water (< 3 mm of thickness, and the beam is focused inside this layer of water). At low laser intensity, one can see that the transmission remains constant (at a value of $T = 95\%$) for both cases, and it starts to drop quickly around 10 GW/cm² for the thin water layer setup ($T = 75\%$), while it remains unchanged for the WTC case.

Furthermore, with the WTC setup, the drop is repelled to around 20 GW/cm² ($T = 90\%$ while $T = 50\%$ for the thin layer case).

The transmission measurements for the thin water layer setup are in agreement with previous measurements that stated a breakdown threshold at around 10 GW/cm² for green wavelength in the ns regime. As expected, the saturating behavior of the transmitted energy after reaching the threshold is visible. However, in the case of the water tank, we can clearly see that the transmitted energy does not change before 20 GW/cm², and then it starts to drop, indicating a breakdown behavior inside the water. Thus, the WTC allows to transmit higher intensity than with the thin layer of water before the breakdown.

Hence, the threshold has been doubled (20 GW/cm² instead of 10 GW/cm²).

B. Pulse duration measurements

The pulse duration [full width at half maximum (FWHM)] of the laser pulse passing through water has been measured with the method described above and is plotted in Fig. 4.

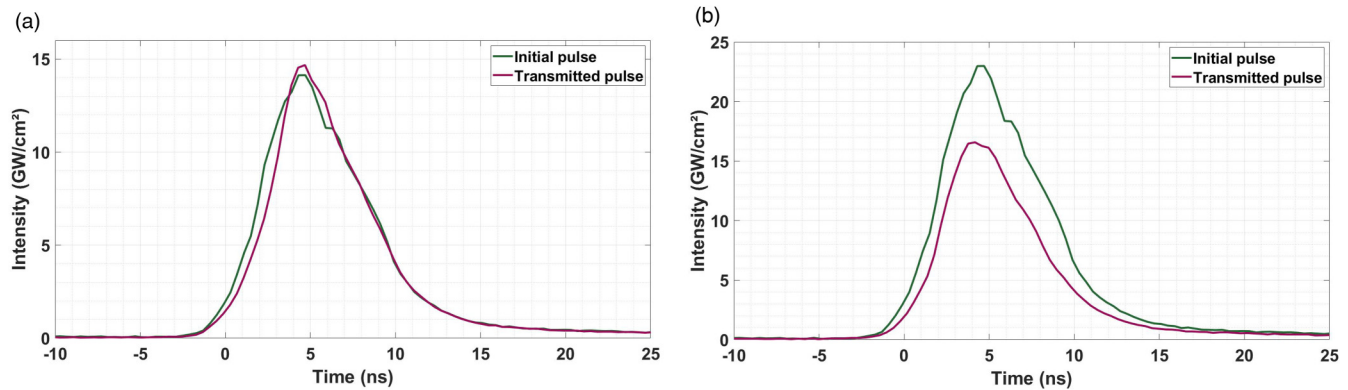


FIG. 5. Initial and transmitted laser pulse through the water tank for two intensities: 14 GW/cm² (left) and 23 GW/cm² (right).

TABLE I. Attenuation (δP in GPa) calculated by the Finite Element code (Abaqus).

Pressure loading (GPa)	50 μm (GPa)	150 μm (GPa)	500 μm (GPa)	1 mm (GPa)
4	0.2	0.75	1.56	2.32
6	0.2	1	2.19	3.45
8	0.3	1.2	2.83	4.15
10	0.35	1.4	3.53	5.25
12	0.45	1.5	4.1	6.37

The values for the FWHM of the laser pulse range from 7.4 to 6.7 ns below 10 GW/cm² in both thin and thick water cases. This first slow decrease in the pulse duration could originate from different sources like a breakdown at the end of the laser pulse. However, the pulse duration rapidly decreases from 6.7 ns at 10 GW/cm² to 4.5 ns at 20 GW/cm² for the case of the thin layer of water, while it remains constant (6.6 ns at 10 GW/cm²) and starts to drop at only 16 GW/cm² for the WTC (6.2 ns at 20 GW/cm²). This sharp decrease in the pulse width indicates that a breakdown has occurred. Indeed, when the breakdown plasma is initiated, the beginning of the laser pulse (until the breakdown is created) has not been absorbed, while the remaining part starts being absorbed. As a consequence, its total duration is reduced.

Furthermore, initial laser pulse and transmitted laser pulse (measured with the photodiode, after the water tank) are plotted in Fig. 5 for 14 and 23 GW/cm². Consistent with other measurements, we can see that there is no breakdown for the 14 GW/cm² pulse as it remains unchanged compare to the initial laser pulse. However, we can see that the transmitted pulse is weaker (16 GW/cm² instead of 23 GW/cm²) and shorter (6 ns instead of 6.8 ns) in the case of an intensity of 23 GW/cm², indicating that a breakdown occurred.

C. Pressure measurements with VISAR

A VISAR has been used to measure the rear-free surface velocity of pure aluminum (99.9%) target immersed under water. As material parameters (density, elastic stiffness, etc.) are well-known

for pure aluminum, hence the plasma pressure obtained from shock waves measurement is very precise.

Thus, through the temporal velocity profile of the rear surface, one can calculate the related rear pressure. Then, Finite Element simulations of the specimen response are used to calculate the attenuation of the shockwave during its propagation. A Johnson–Cook rheological model was used with the commercial Finite Element code Abaqus, as presented in previous work.¹⁷

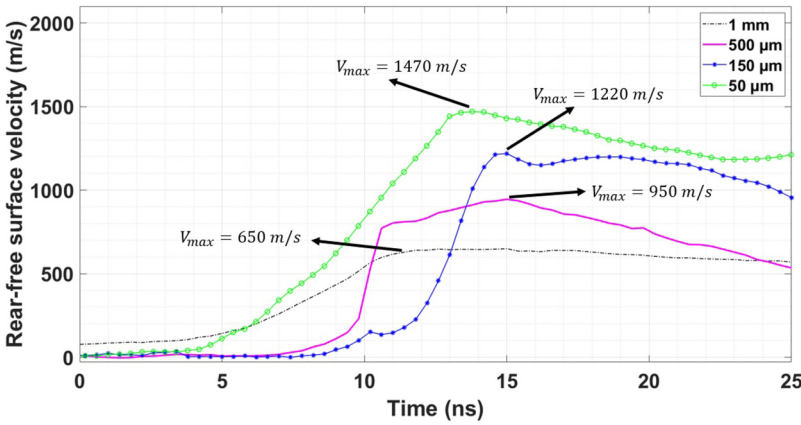
Afterall, one can extract the plasma pressure (at the front face of the specimen) from the rear shock wave pressure measured by adding the known attenuation, for the given used thickness. Indeed, as the shock wave propagates, it will be attenuated mainly by the release wave, behind the shock wave, which travels faster. Various aluminum target thicknesses were chosen (50 μm , 150 μm , 500 μm , and 1 mm) in order to verify the consistency of each measurement with the estimated plasma pressure. This procedure also allows verifying that the estimated attenuation was correct. Values of attenuation (δP) for different pressure and different thicknesses are given in Table I.

The plasma maximum pressure as a function of the maximum rear-free velocity surface is given by Ref. 15,

$$P_{max} = \rho_0 \left(C_0 + S \frac{v_{max}}{2} \right) \frac{v_{max}}{2} + \delta P + \frac{2\sigma_{y0}}{3}, \quad (1)$$

where $\rho_0 = 2700 \text{ kg/m}^3$ is the material density, $C_0 = 5380 \text{ m/s}$ is the bulk speed of sound, $S = 1.38$ is the Hugoniot constant, δP is the attenuation, $\sigma_{y0} = 154 \text{ MPa}$ is the yield strength, and v_{max} is the maximum rear-free surface velocity measured by the VISAR.

Four velocity profiles obtained at 22 GW/cm² for each thickness are plotted in Fig. 6. Velocities reach high values (1470 m/s for a 50 μm Al foil, 1220 m/s for 150 μm , 950 m/s for 500 μm , and 650 m/s for 1 mm), even though they decrease for higher thickness due to higher attenuation as shown in Table I. The maximum reached velocity during the shock can be clearly measured and lies with the maximum plasma pressure according to Eq. (1). All velocities lead to plasma pressure in the 10–13 GPa pressure range (13.18 GPa for 50 μm , 11.98 GPa for 150 μm , 11.71 GPa for 500 μm , and 11.04 GPa for 1 mm).

**FIG. 6.** Rear-free surface velocity (m/s) measured after laser shock for four thicknesses of the aluminum target (0.05, 0.15, 0.5, and 1 mm).

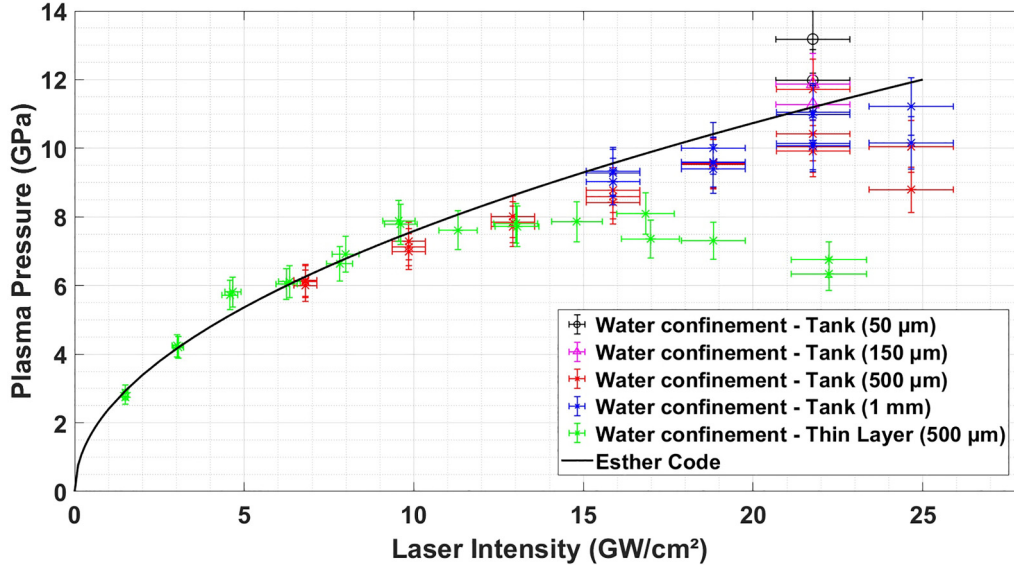


FIG. 7. Maximum plasma pressure (GPa) as a function of the laser intensity (GW/cm^2) for four aluminum thicknesses (0.05, 0.15, 0.5, and 1 mm) and for the two configurations, WTC and thin water layer. Comparison with numerical simulations from Esther Code.¹⁸

Figure 7 shows the pressure obtained by the same method for various laser intensities and for the two configurations: The WTC (for four aluminum target thicknesses: 50, 150, 500, and 1 mm) and the thin water layer configuration ($500 \mu\text{m}$ target).

We have also plotted in Fig. 7 numerical result obtained with the Esther Code, CEA,¹⁸ showing the pressure as a function of intensity. Esther is a one-dimensional Lagrangian code, which calculates the absorption of the laser by the plasma and hydrodynamics phenomena associated. However, breakdown mechanisms are not implemented in Esther Code so that the simulated pressure will not saturate.

In the case of a classical thin layer of water, pressure is increasing up to 8 GPa at $10 \text{ GW}/\text{cm}^2$. For higher intensity, one can see that pressure does not increase anymore but instead decreases slightly. However, for the case of the WTC, the pressure is still increasing above $10 \text{ GW}/\text{cm}^2$ and reaches much higher pressures close to 12 GPa at $22 \text{ GW}/\text{cm}^2$. For higher intensities ($>24 \text{ GW}/\text{cm}^2$), the pressure starts to saturate and then to decrease, which points out that the breakdown threshold has been reached. It is worth remarking that below the breakdown threshold, measured pressures are very close to the numerical estimations provided by Esther Code.

D. Breakdown threshold

Table II shows an overview of the breakdown threshold values determined through each of our experiments and compared with earlier published works. Even if Refs. 12 and 13 concern a case at 6 ns pulse duration (while we used 7.2 ns), it is important to note that it is very consistent with our results. Indeed, we can globally estimate a threshold value of $20 \text{ GW}/\text{cm}^2$, while previous

experiments stated it to be at $30 \text{ GW}/\text{cm}^2$ and simulations estimated it to be between 6 and $41 \text{ GW}/\text{cm}^2$.

IV. LSP PROCESS CONFIGURATION

A. Experimental setup

During laser shock at high pressures, the aluminum target undergoes plastic deformation that can be evidenced by a distortion of its top surface as illustrated in Fig. 8. This surface sinking was measured with a Dektak 150 (Bruker) contact profilometer. There is also a descent of the sample's surface, which is induced by laser ablation; previous work has stated that this ablation is also proportional to the laser intensity, and most importantly, for intensities involved in laser shock processes, this ablation is negligible compared to the plastic deformation.¹⁹

However, as a single laser shot does not create a deep enough sinking of the material to enable a precise characterization with the used profilometer, we instead performed an LSP treatment (multiple shots) on samples on a large area of $1 \times 1 \text{ cm}^2$.

TABLE II. Breakdown threshold values obtained with our different experiments and comparison with earlier published works (at 6 ns pulse duration).

Experiment	I_{th} (GW/cm^2)	I_{th}^{12} (GW/cm^2)	I_{th}^{13} (GW/cm^2)
Energy transmission	22	30	—
Pulse duration	18	—	—
Pressure	24	—	—
Simulation	—	—	6–41

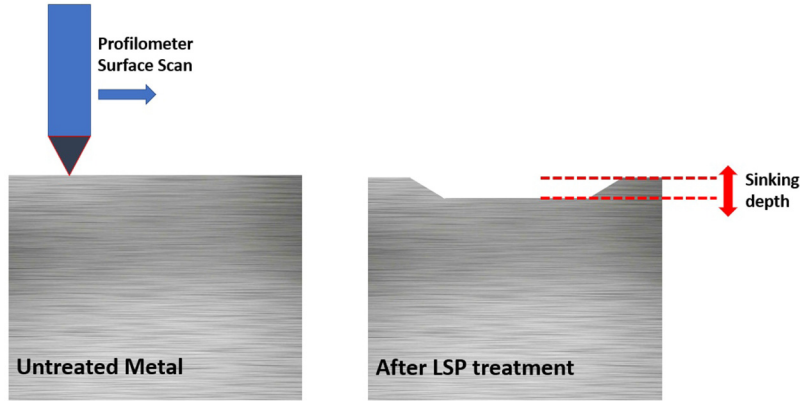


FIG. 8. Sinking measurement method.

The method used to measure the specimen surface sinking after LSP treatment is shown in Fig. 8.

For that purpose, we used samples made of an aluminum alloy (Al-2024) immersed under water combined with another setup where the focal lens is also immersed under water. The sample is attached under water, at the focal point. This whole setup, except the focal lens that stays fixed, is itself attached on a two-axis motorized stage. The displacement of the stage, while the laser beam remains fixed and operated continuously at a frequency of 2 Hz, allows to treat a large patch on the aluminum sample (10 mm by 10 mm). We shot at a high overlapping ratio of 1800%. The spot size was chosen as 1 mm since our multishot setup does not allow us to use a DOE (as the lens is immersed inside the water to avoid water projection between two shots). However, with smaller laser spot, the diffraction effect contribution to the spatial distribution of energy is almost negligible. Indeed, these small spots, obtained close to the focal plane, correspond to a far field imaging (which is equivalent to a long distance propagation of the beam). In our case (1 mm spot size and +250 mm focal lens), we have a total beam propagation of 13 m (8 m from the source to the lens, plus 5 m of equivalent propagation when imaging the beam). Consequently, diffraction effects are then move out of the considered main spot as they are associated with various angles that transform into important distances in far field.

Hence, one can consider the beam to be homogeneous with no over-intensities, thus not initiating prematurely a breakdown inside water, as shown in Fig. 9.

B. Results: Deformation of the target surface

Nine samples were treated with the same parameters (1 mm focal spot, 7.2 ns pulse duration, 532 nm wavelength, and a pulse density equal to $p = 2300$ pulses/cm², with $p = 1/D^2$, with D being the displacement of the laser spot between two consecutive shots), but with different laser intensities. Intensities were increased from 4 GW/cm² to more than 20 GW/cm². As explained above, this leads to a permanent deformation (sinking) of the upper target surface due to plastic strain. As we expect the sinking to be proportional to the pulse density and to the plasma pressure, we should see a saturation of the sinking when the breakdown occurs since the laser intensity will stop to increase (as it will be for the pressure).²⁰

Figure 10 shows the sinking measurements as a function of laser intensity.

The peak-to-peak value of sinking almost linearly increases from 60 μm at 6 GW/cm² to 220 μm at 22 GW/cm², with no saturation nor slope reduction after 10 GW/cm². Hence, we can expect that no breakdown has occurred in the range of 6–22 GW/cm².

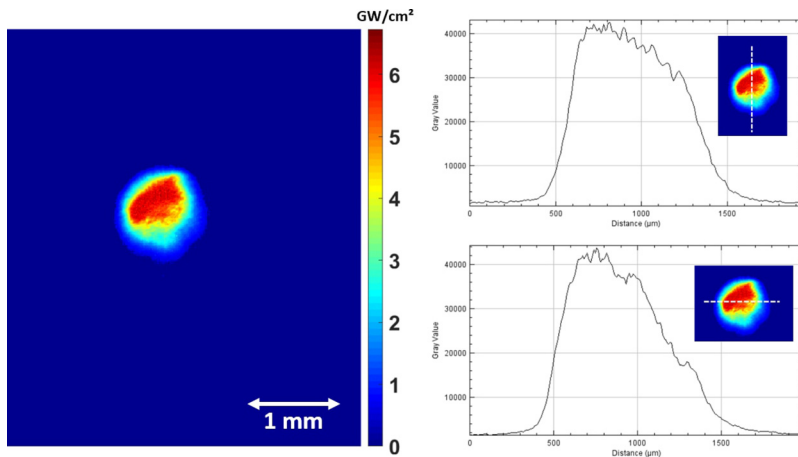


FIG. 9. Spatial distribution of intensity ($I_{\text{mean}} = 4$ GW/cm²) for our 1 mm spot size without DOE.

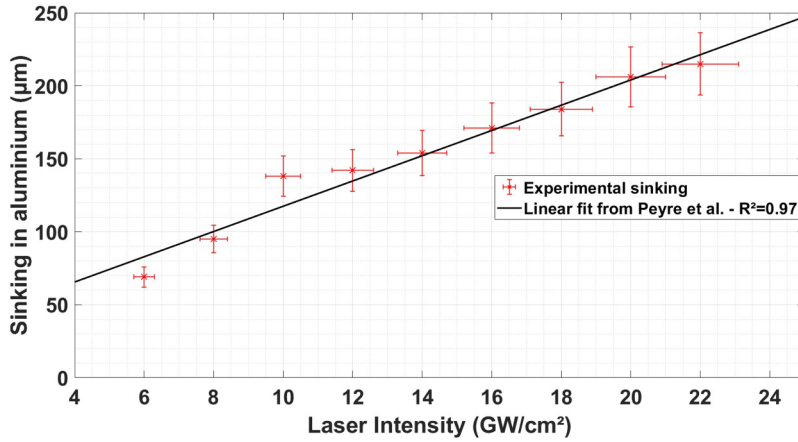


FIG. 10. Sinking of the aluminum target surface (μm) as a function of the laser intensity (GW/cm^2) for a pulse density of 2300 pulses per cm^2 and a spot size of 1 mm. The linear fitting law comes from Peyre *et al.*²¹

Furthermore, these results are consistent with a previous work of Peyre *et al.*²¹ Indeed, the surface deformation e induced by a single laser shot was found to be a function of the maximum applied pressure at square: $e = f(P_{\text{max}}^2)$. Thus, as $P_{\text{max}} \propto \sqrt{I}$, the deformation is expected to be linearly increasing with the intensity. This linear dependency can clearly be seen in Fig. 10 up to $20 \text{ GW}/\text{cm}^2$, confirming that the intensity irradiating the target has not decreased due to a breakdown.

Altogether, this configuration that is close to industrial LSP treatment has also confirmed that the breakdown threshold is higher when we ensure that no breakdown occurred at the surface of the confinement.

V. CONCLUSION

A. Increase in the water breakdown threshold

Our results demonstrate that the breakdown threshold of water is higher when it occurs in the depth of the water compared to when it occurs at the surface of the water. This breakdown threshold is not dependent on the water thickness (it only depends on if it is initiated at the surface or in the volume), but it requires a minimum thickness of water to ensure that the threshold at the target (in volume, around $24 \text{ GW}/\text{cm}^2$) is reached before the threshold at the surface ($10 \text{ GW}/\text{cm}^2$) is reached. This minimum thickness can be calculated as a function of the numerical aperture of the used setup; however, using a great thickness of about 10 cm ensures that this condition is attained. The true ability of using our proposed water tank configuration is to move the water breakdown phenomena from its surface to its volume, where the threshold is approximately 2 times higher. Thus, the pressure is increased by 50%.

B. Prospects for LSP

As this new configuration repels the maximum possible pressure to 12 GPa from 6 to 8 GPa, it should now help in treating either new materials with very high yield strength or treating them at a larger depth. Indeed, materials experience plastic deformation after the pressure exceeds the Hugoniot Elastic Limit (HEL), and

this plastic deformation will saturate after twice the HEL has been reached.²² As HEL is proportional to the elasticity limit of the material, some steels or titanium alloy can reach an HEL greater than 3 GPa²³ so that an optimal pressure loading should be close to 10 GPa. On more standard materials, a higher pressure allows generating a plastic strain at larger depth which is often beneficial, e.g., for fatigue loading resistance.

C. Prospects for high-pressure applications

Pressures generated under the WCR with a thin water film cannot exceed 8 GPa as already underlined. Therefore, to go to higher pressures, one has to use the direct ablation regime [DAR (Ref. 24)] that requires heavier and expensive laser systems. Moreover, DAR is also harder to implement since vacuum is required to avoid air breakdown. Previous experiments and simulations¹⁸ estimated that a laser intensity of more than $400 \text{ GW}/\text{cm}^2$ is required in direct ablation to reach pressures above 10 GPa. This is almost 20 times higher than in the WTC presented in this article; thus, very high energy systems (up to 200 J) would be required instead of the 14 J source used here with the WTC.

D. Summary and future work

We developed a new configuration (water tank configuration) for laser induced plasma applications under the water confinement regime. This configuration aims to significantly increase the plasma breakdown threshold. The breakdown threshold intensity was increased from around 8 to $20 \text{ GW}/\text{cm}^2$ for the case of a 7 ns laser pulse at 532 nm. Thresholds were experimentally confirmed from the energy and the duration of the transmitted pulses. The demonstrated work also covers pressure measurements and deformation (sinking) of the target surface.

Using this new configuration, one now should be able to reach very high pressure (up to 12 GPa) without using a heavy and costly laser system nor expensive setups with vacuum for direct ablation creation. As a consequence, this will open the path for the treatment of a very high yield strength material by laser shock peening.

Future works should focus on the physical mechanism by which the breakdown threshold is different on the water surface or in volume.

ACKNOWLEDGMENTS

This research was funded by Thales Company, institutions (CEA, CNRS, and ENSAM), and by the ANR (Agence Nationale de la Recherche), Forge Laser Project (Grant No. ANR-18-CE08-0026).

DATA AVAILABILITY

The data that support the findings of this study are available from the corresponding author upon reasonable request.

REFERENCES

- ¹P. Peyre, R. Fabbro, P. Merrien, and H. P. Lieurade, "Laser shock processing of aluminium alloys. Application to high cycle fatigue behaviour," *Mater. Sci. Eng., A* **210**, 102–113 (1996).
- ²H. Jasim, A. Demir, B. Previtali, and Z. Taha, "Process development and monitoring in stripping of a highly transparent polymeric paint with ns-pulsed fiber laser," *Opt. Laser Technol.* **93**, 60–66 (2017).
- ³M. Sagnard, R. Ecalt, F. Touchard, M. Boustie, and L. Berthe, "Development of the symmetrical laser shock test for weak bond inspection," *Opt. Laser Technol.* **111**, 644–652 (2018).
- ⁴C. Phipps, J. Luke, and W. Helgeson, "Laser space propulsion overview," *Proc. SPIE* **6606**, 660602 (2007).
- ⁵N. C. Anderholm, "Laser-generated stress waves," *Appl. Phys. Lett.* **16**, 113–115 (1970).
- ⁶R. Fabbro, J. Fournier, P. Ballard, D. Devaux, and J. Virmont, "Physical study of laser-produced plasma in confined geometry," *J. Appl. Phys.* **68**, 775–784 (1990).
- ⁷L. Berthe, R. Fabbro, P. Peyre, L. Tollier, and E. Bartnicki, "Shock waves from a water-confined laser-generated plasma," *J. Appl. Phys.* **82**, 2826–2832 (1998).
- ⁸A. Sollier, L. Berthe, and R. Fabbro, "Numerical modeling of the transmission of breakdown plasma generated in water during laser shock processing," *Eur. Phys. J. Appl. Phys.* **16**, 131–139 (2001).
- ⁹L. Berthe, R. Fabbro, P. Peyre, and E. Bartnicki, "Wavelength dependent of laser shock-wave generation in the water-confinement regime," *J. Appl. Phys.* **85**, 7552–7555 (1999).
- ¹⁰F. Docchio, C. Sacchi, and J. Marshall, "Experimental investigation of optical breakdown thresholds in ocular media under single pulse irradiation with different pulse durations," *Laser Ophthalmol.* **1**, 83–93 (1986).
- ¹¹A. Sollier, L. Berthe, P. Peyre, E. Bartnicki, and R. Fabbro, *Proc. SPIE* **4831**, 463–467 (2003).
- ¹²A. Vogel, K. Nahen, D. Theisen, and J. Noack, "Plasma formation in water by picosecond and nanosecond nd:yag laser pulses—part I: Optical breakdown at threshold and superthreshold irradiance," *IEEE J. Sel. Top. Quantum Electron.* **2**, 847–860 (1996).
- ¹³H. Zhang, J. Lu, X. Ni, and Z. Shen, "Numerical simulation for laser-induced breakdown thresholds and plasma formation in water," *Chin. Opt. Lett.* **3**, S100–S102 (2005).
- ¹⁴L. Barker and R. Hollenbach, "Laser interferometer for measuring high velocities of any reflecting surface," *J. Appl. Phys.* **43**, 4669–4675 (1972).
- ¹⁵R. Fabbro, P. Peyre, L. Berthe, and X. Scherpereel, "Physics and applications of laser-shock processing," *J. Laser Appl.* **10**, 265–279 (1998).
- ¹⁶C. Le Bras *et al.*, "Laser shock peening: Toward the use of pliable solid polymers for connement," *Metals* **9**, 1–13 (2019).
- ¹⁷A. Rondepierre *et al.*, "Beam size dependency of a laser-induced plasma in confined regime: Shortening of the plasma release. Influence on pressure and thermal loading," *Opt. Laser Technol.* **135**, 106689 (2021).
- ¹⁸S. Bardy *et al.*, "Development of a numerical code for laser-induced shock waves applications," *Opt. Laser Technol.* **124**, 105983 (2020).
- ¹⁹A. Sollier, "Etude des plasmas générés par interaction laser-matière en régime confiné: Application au traitement des matériaux par choc laser," Ph.D. thesis (Université de Versailles St-Quentin, 2002), thèse de doctorat dirigée par Fabbro, Rémy Physique Versailles-St Quentin en Yvelines, 2002.
- ²⁰P. Ballard, J. Fournier, R. Fabbro, J. Frelat, and L. Castex, "Study of the plastification of metallic targets shocked by a laser pulse of high energy," *J. Phys.* **49**, 401–406 (1988).
- ²¹P. Peyre, L. Berthe, V. Vignal, I. Popa, and T. Baudin, "Analysis of laser shock waves and resulting surface deformations in an Al–Cu–Li aluminum alloy," *J. Phys. D: Appl. Phys.* **45**, 335304 (2012).
- ²²P. Ballard, J. Fournier, R. Fabbro, and J. Frelat, "Residual stresses induced by laser-shocks," *J. Phys. IV* **1**, 487–494 (1991).
- ²³K. Ahn, H. Huh, and L. Park, "Comparison of dynamic hardening equations for metallic materials with three types of crystalline structures," in *5th International Conference on High Speed Forming, Dortmund, Germany, 24–26 April* (ICHSE, Dortmund, 2012).
- ²⁴C. Phipps *et al.*, "Impulse coupling to targets in vacuum by KrF, HF, and CO₂ single-pulse lasers," *J. Appl. Phys.* **64**, 1083–1096 (1988).